JAEA-Technology
2008-003

Preliminary Analyses on Hydrogen Diffusion through Small Break of Thermo-chemical IS Process Hydrogen Plant

Marketa SOMOLOVA*, Atsuhiko TERADA, Hiroaki TAKEGAMI and Jin IWATSUKI

IS Process Technology Group
Nuclear Science and Engineering Directorate

December 2008

Japan Atomic Energy Agency
日本原子力研究開発機構

JAEA-Technology

Preliminary Analyses on Hydrogen Diffusion through Small Break of Thermo-chemical IS Process Hydrogen Plant

Marketa SOMOLOVA*, Atsuhiko TERADA, Hiroaki TAKEGAMI and Jin IWATSUKI

Nuclear Applied Heat Technology Division
Nuclear Science and Engineering Directorate
Japan Atomic Energy Agency
Oarai-machi, Higashiibaraki-gun, Ibaraki-ken

(Received January 7, 2008)

Japan Atomic Energy Agency has been conducting a conceptual design study of nuclear hydrogen demonstration plant, that is, a thermo-chemical IS process hydrogen plant coupled with the High temperature Engineering Test Reactor (HTTR-IS), which will be planed to produce a large amount of hydrogen up to 1000m^3/h. As part of the conceptual design work of the HTTR-IS system, preliminary analyses on small break of a hydrogen pipeline in the IS process hydrogen plant was carried out as a first step of the safety analyses. This report presents analytical results of hydrogen diffusion behaviors predicted with a CFD code, in which a diffusion model focused on the turbulent Schmidt number was incorporated. By modifying diffusion model, especially a constant accompanying the turbulent Schmidt number in the diffusion term, analytical results was made agreed well with the experimental results.

Keywords: Hydrogen, Diffusion, Small Break, Turbulent Schmidt Number, Analyses

* Nuclear Research Institute Rez plc (JAEA Foreign Researcher Inviting Program)

JAEA-Technology　2008-003

熱化学法 IS プロセス水素製造プラントにおける小口径破断による水素拡散予備解析

日本原子力研究開発機構　原子力基礎工学研究部門
核熱応用工学ユニット

Marketa SOMOLOVA*、寺田　敦彦、竹上　弘彰、岩月　仁

(2008 年 1 月 7 日　受理)

日本原子力研究開発機構では、高温工学試験研究炉（HTTR）に熱化学法 IS プロセス水素製造プラントを接続して最高 1000m³の水素を製造する原子力水素実証プラント（HTTR-IS）の概念設計研究を進めている。HTTR-IS の概念設計の一環として、IS プロセスの水素配管の小口径破断の予備解析をおこなった。これは、安全解析評価の第 1 段階となるもので、本報告では、乱流シミュット数に着目した拡散モデルを CFD コードに組み込んで得られた水素拡散挙動の解析結果について述べる。乱流シュミット数に随伴する定数を修正することにより、解析結果を実験結果とよく一致させることができた。

大洗研究開発センター（駐在）：　〒311-1393　茨城県東茨城郡大洗町成田町 4002
* チェコ原子力研究所（外国人研究者招聘制度）

Contents

目　次

1. Introduction

It is universally admitted that hydrogen is one of the best energy media to alleviate the global warming problem, and its demand will increase greatly in the near future. However, there is a problem about how to produce a large amount of the hydrogen economically while reducing CO_2 emission. Hydrogen production with nuclear heat of a high-temperature gas-cooled reactor (HTGR) is one of the solutions.

Japan Atomic Energy Agency has been conducting a conceptual design study of nuclear hydrogen demonstration plant, that is, a thermo-chemical IS process hydrogen plant coupled with the High temperature Engineering Test Reactor (HTTR-IS), which will be planed to produce a large amount of hydrogen up to 1000m^3/h [1]. One of the most important safety design issues for an HTGR hydrogen production system is to ensure reactor safety against fire and explosion accidents because a large amount of combustible fluid is dealt with near the reactor in the system. A number of experiments and analyses was made considered hydrogen release and dispersion, fire and explosions. Representative literatures [2-8] are summarized in Appendix.

As part of the conceptual design work of the HTTR-IS system, preliminary analyses on small break of a hydrogen pipeline in the IS process hydrogen plant was carried out as a first step of the safety analyses. The objective of the work described in this report is to confront 2D FLUNENT code and experiments benchmark calculation for the case of hydrogen jet diffusion which may occur during possible hydrogen plant accident. The existing model for the calculation of this case was used and modified (for better accuracy) by changing the constant of turbulent diffusion term including turbulent Schmidt number. This report presents analytical results of hydrogen diffusion behaviors predicted with the CFD code.

2. Analytical model and conditions

The problem considers the calculation of hydrogen jet diffusion that may occur during possible hydrogen plant accident. Figure 2.1 shows the 2D geometry used for the calculation. The computational grid was created in the ANSYS ICEM program and after that the mesh was adapted in FLUNENT 6.3 code using gradient of static pressure (see the Figure 2.2) [9]. Hydrogen jet leaks out from a nozzle with diameter d = 12.7 mm and length L_s = 50 mm. Its total pressure is 40.1 MPa and temperature 300 K. Hydrogen is dispersed into the space (D = 2,000 mm, L = 10,000 mm) containing air in ambient conditions (total pressure 0.1 MPa, temperature 300 K).

For the calculation were used the following governing equations [10].

(1) Transport Equations for the Realizable k-ε model

The Reynolds-averaged approach to turbulence modeling requires that the Reynolds stress be appropriately modeled. A common method employs the Boussinesq hypothesis to relate the Reynolds stress to the mean velocity gradients:

$$-\rho\overline{u_i'u_j'} = \mu_t\left(\frac{\partial u_i}{\partial x_j}+\frac{\partial u_j}{\partial x_i}\right)-\frac{2}{3}\left(\rho k+\mu_t\frac{\partial u_k}{\partial x_k}\right)\delta_{ij} \tag{2.1}$$

The realizable k-ε model is a relatively recent development. The term “realizable” means that the model satisfies certain mathematical constraints on the Reynolds stress, consistent with the physics of turbulent flows. An immediate benefit of the realizable k-ε model is that it more accurately predicts the spreading rate of both planar and round jets. It is also likely to provide superior performance for flows involving rotation, boundary layers under strong adverse pressure gradients, separation, and recirculation.

The modeled transport equations for k and ε in the realize k-ε model are

$$\frac{\partial}{\partial t}(\rho k)+\frac{\partial}{\partial x_j}(\rho k u_j)=\frac{\partial}{\partial x_j}\left[\left(\mu+\frac{\mu_t}{\sigma_k}\right)\frac{\partial k}{\partial x_j}\right]+G_k+G_b-\rho\varepsilon-Y_M+S_k \tag{2.2}$$

and

$$\frac{\partial}{\partial t}(\rho \varepsilon)+\frac{\partial}{\partial x_j}(\rho \varepsilon u_j)=\frac{\partial}{\partial x_j}\left[\left(\mu+\frac{\mu_t}{\sigma_\varepsilon}\right)\frac{\partial \varepsilon}{\partial x_j}\right]+\rho C_1 S\varepsilon-\rho C_2\frac{\varepsilon^2}{k+\sqrt{\nu\varepsilon}}+C_{1\varepsilon}\frac{\varepsilon}{k}C_{3\varepsilon}G_b+S_\varepsilon \tag{2.3}$$

where

$$C_1 = \max\left[0.43, \frac{\eta}{\eta+5}\right], \quad \eta = S\frac{k}{\varepsilon} \quad , \quad S = \sqrt{2S_{ij}S_{ij}} \tag{2.4}$$

The eddy viscosity is computed from

$$\mu_t = \rho C_\mu \frac{k^2}{\varepsilon} \tag{2.5}$$

$$C_\mu = \frac{1}{A_0 + A_s \dfrac{kU^*}{\varepsilon}} \tag{2.6}$$

$$U^* = \sqrt{S_{ij}S_{ij} + \tilde{\Omega}_{ij}\tilde{\Omega}_{ij}} \tag{2.7}$$

and

$$\tilde{\Omega}_{ij} = \overline{\Omega}_{ij} \quad , \overline{\Omega}_{ij} = \frac{1}{2}\left(\frac{\partial u_i}{\partial x_j} - \frac{\partial u_j}{\partial x_i}\right) \tag{2.8}$$

where $\overline{\Omega}_{ij}$ is the mean rate-of-rotation tensor viewed in a rotating reference frame with the angular velocity ω_k. The model constants A_0 and A_s are given by

$$A_0 = 4.04 \quad , \quad A_s = \sqrt{6}\cos\phi \tag{2.9}$$

where

$$\phi = \frac{1}{3}\cos^{-1}\left(\sqrt{6}W\right) \tag{2.10}$$

$$W = \frac{S_{ij}S_{jk}S_{ki}}{\tilde{S}^3} \tag{2.11}$$

$$\tilde{S} = \sqrt{S_{ij}S_{ij}} \tag{2.12}$$

$$S_{ij} = \frac{1}{2}\left(\frac{\partial u_j}{\partial x_i} + \frac{\partial u_i}{\partial x_j}\right) \tag{2.13}$$

The model constants are as follows:

$$C_{1\varepsilon} = 1.44, C_2 = 1.9, \sigma_k = 1.0, \sigma_\varepsilon = 1.2 \tag{2.14}$$

G_k represents the generation of turbulence kinetic energy due to the mean velocity gradients, G_b is the generation of turbulence kinetic energy due to buoyancy, Y_M represents the contribution of the fluctuating dilatation in compressible turbulence to the overall dissipation rate, C_2 and $C_{1\varepsilon}$ are constants, σ_k and σ_ε are the turbulent Prandtl numbers for K and ε.

The term G_k is modeled identically for the standard, RNG, and realizable k-ε models. From the exact equation for the transport of k, this term may be defined as

$$G_k = -\rho \overline{u_i' u_j'} \frac{\partial u_j}{\partial x_i} \tag{2.15}$$

To evaluate G_k in a manner consistent with the Boussinesq hypothesis,

$$G_k = \mu_t S^2 \tag{2.16}$$

Where S is the modules of the mean rate-of-strain tensor, defined as

$$S = \sqrt{2 S_{ij} S_{ji}} \tag{2.17}$$

For high-Mach-number flows, compressibility affects turbulence through so-called “dilatation dissipation”, which is normally neglected in the modeling of incompressible flows.

$$Y_M = 2\rho\varepsilon M_t^{\ 2} \tag{2.18}$$

where M_t is the turbulent Mach number, defined as

$$M_t = \sqrt{\frac{k}{a^2}} \tag{2.19}$$

where a(= $\sqrt{\gamma RT}$) is the speed of sound.

(2) Species transport

$$\frac{\partial}{\partial t}\left(\rho Y_i\right)+\frac{\partial}{\partial x_j}\left(\rho u_j Y_i\right)=-\frac{\partial J_{i,j}}{\partial x_j} \tag{2.20}$$

where Y_i represents the local mass fraction of each species and J_i is the diffusion flux of species i.

$$J_{i,j}=-\left(\rho D_{m,i}+\frac{\mu_t}{Sc_t}\right)\frac{\partial Y_i}{\partial x_j}-\frac{D_{T,i}}{T}\frac{\partial T}{\partial x_i} \quad , \quad Sc_t=0.7 \tag{2.21}$$

where Sc_t is the effective Schmidt number [11] and $D_{m,i}$ is the diffusion coefficient in the mixture, and $D_{T,i}$ is the thermal diffusion coefficient.

$$D_{T,i}=-2.59\times 10^{-7}T^{41.659}\left[\frac{M_{w,i}^{0.511}X_i}{\sum_{i=1}^{N}M_{w,i}^{0.511}X_i}-Y_i\right]\cdot\left[\frac{\sum_{i=1}^{N}M_{w,i}^{0.511}}{\sum_{i=1}^{N}M_{w,i}^{0.489}X_i}\right] \tag{2.22}$$

(3) Energy calculation

$$\frac{\partial}{\partial t}\left(\rho E\right)+\frac{\partial}{\partial x_i}\left(u_i\left(\rho E+p\right)\right)=\frac{\partial}{\partial x_j}\left(k_{eff}\frac{\partial T}{\partial x_j}-\sum_j h_j J_j+u_i\left(\tau_{ij}\right)_{eff}\right) \tag{2.23}$$

$$E=h-\frac{p}{\rho}+\frac{u_i^{\,2}}{2} \tag{2.24}$$

$$h=\sum_j Y_j h_j \tag{2.25}$$

$$h_j=\int_{T_{ref}}^{T}c_{p,j}\,dT \tag{2.26}$$

$$k_{eff}=k+\frac{C_p\mu_t}{\Pr_t} \quad , \quad \Pr_t=0.85 \tag{2.27}$$

where E is the total energy, k_{eff} is the effective thermal conductivity, and $(\tau_{ij})_{eff}$ is the deviatoric stress tensor, defined as

$$\left(\tau_{ij}\right)_{eff} = \mu_{eff}\left(\frac{\partial u_j}{\partial x_i}+\frac{\partial u_i}{\partial x_j}\right)-\frac{2}{3}\mu_{eff}\frac{\partial u_k}{\partial x_k}\delta_{ij} \tag{2.28}$$

(4) Mass conservation equation

$$\frac{\partial \rho}{\partial t}+\frac{\partial}{\partial x_j}\left(\rho u_j\right)=0 \tag{2.29}$$

(5) Momentum conservation equations

$$\frac{\partial \rho}{\partial t}+\frac{\partial}{\partial x_j}\left(\rho u_j u_i\right)=-\frac{\partial p}{\partial x_i}+\frac{\partial}{\partial x_j}\left[\mu\left(\frac{\partial u_i}{\partial x_j}+\frac{\partial u_j}{\partial x_i}-\frac{2}{3}\delta_{ij}\frac{\partial u_i}{\partial x_j}\right)\right]+\frac{\partial}{\partial x}\left(-\rho\overline{u_i' u_j'}\right) \tag{2.30}$$

where p is the static pressure.

Fluid materials – hydrogen, nitrogen, and oxygen – were defined as in Tables 2.1, 2.2 and 2.3 respectively. The air was considered as a mixture of nitrogen and oxygen (nitrogen mass fraction: 0.77 $kg.kg^{-1}$, oxygen mass fraction: 0.23 $kg.kg^{-1}$).

Next material properties were defined as follows:

(6) Density (compressible flow)

For compressible flows, the gas law is as following:

$$\rho = \frac{p}{RT\sum_i \frac{Y_i}{M_{w,i}}} \tag{2.31}$$

where p is the local relative pressure, R is the universal gas constant, Y_i is the mass fraction of species i, and $M_{w,i}$ is the molecular weight of species i.

(7) Specific heat capacity

Mixture's specific heat capacity as a mass fraction average of the pure species best capacities:

$$c_p = \sum_i Y_i c_{p,i} \tag{2.32}$$

Pure component's specific heat capacity is a function of temperature.

(8) Viscosity

$$\mu = \sum_i \frac{X_i \mu_i}{\sum_j X_i \varphi_{ij}} \tag{2.33}$$

where

$$\phi_{ij} = \frac{\left[1 + \left(\frac{\mu_i}{\mu_j}\right)^{1/2} \left(\frac{M_{w,i}}{M_{w,j}}\right)^{1/4}\right]^2}{\left[8\left(1 + \frac{M_{w,i}}{M_{w,j}}\right)\right]^{1/2}} \tag{2.34}$$

(9) Thermal conductivity

$$k = \sum_i \frac{X_i k_i}{\sum_j X_i \varphi_{ij}} \tag{2.35}$$

where

$$\phi_{ij} = \frac{\left[1 + \left(\frac{\mu_i}{\mu_j}\right)^{1/2} \left(\frac{M_{w,i}}{M_{w,j}}\right)^{1/4}\right]^2}{\left[8\left(1 + \frac{M_{w,i}}{M_{w,j}}\right)\right]^{1/2}} \tag{2.36}$$

3. Results and discussion

A result was created contours of static temperature, pressure, Mach number, turbulent viscosity, and hydrogen concentration (mole fraction). Distributions of each parameter for nozzle pressure 40.1 MPa and for different Schmidt number are shown in Figures 3.1, 3.2, 3.3, 3.4, and 3.5. X – Y plots of hydrogen concentration on the axis in Figure 3.6 came next.

Figure 3.7 and Table 3.1 show the comparison between experimental [10] and calculated values of hydrogen gas concentration. In the experiment, hydrogen was blown from ½ inch nozzle with pressure 40 MPa and for calculation was used a theoretical diffusion equation (see below). The solid line in Figure 3.7 represents experimental results; the dotted and dash lines represent calculated values from FLUENT code with Schmidt number 0.7 and 1.4 respectively. The explosion range for hydrogen is from 4 to 75 vol. %. In this critical area the modified model gave us more accurate data which corresponds better with experimental results (and therefore this model is more reasonable for safety evaluations).

Theoretical diffusion equation

$$\frac{Cx}{C_0} = 5.3 \times \frac{D}{x} \times \left(\frac{M_{x0}}{M_0}\right)^{1/2} \times \left(\frac{P_0}{P_a}\right)^{1/2} \tag{3.1}$$

Hydrogen concentration:

$$C_x = \frac{-b + \sqrt{b^2 - 4c}}{2} \tag{3.2}$$

Coefficients:

$$A = 5.3 \times \frac{D}{x} \times \left(\frac{1}{M_0}\right)^{1/2} \times \left(\frac{P_0}{P_a}\right)^{1/2} \times C_0 \tag{3.3}$$

$$c = -A^2 M_a \tag{3.4}$$

$$b = A^2 \left(M_a - M_0\right) \tag{3.5}$$

where

C_x Hydrogen concentration at the x position

C_0 Hydrogen concentration at the nozzle position (1.0)

D Nozzle diameter (0.0127 m)

M_0 Hydrogen molecular weight at the nozzle position (2.0)

M_a Air average molecular weight (28.966)

M_{x0} Hydrogen average molecular weight on the nozzle center axis

P_0 Static pressure at the nozzle point

P_a Ambient pressure (1.10^5 Pa)

x Distance from the nozzle

4. Conclusion

The current model was found to be not sufficiently accurate to predict hydrogen jet diffusion and therefore the model was modified by changing the constant of turbulent diffusion term including turbulent Schmidt number. The modified model showed a good agreement with the experimental results at lower hydrogen concentration within the explosion range of hydrogen. This modified model is thought to be applicable to a general in hydrogen plant safety analysis.

Acknowledgements

The author would like to express my gratitude for support and encouragement to Dr. Shusaku Shiozawa and to Dr. Ryutaro Hino for professional suggestions and comments.

References

[1] N.Sakaba, S. Kasahara, H. Ohashi, H. Sato, S. Kubo, A. Terada, T. Nishihara, K. Onuki, K. Kunitomi, Hydrogen production by using heat from high-temperature gas-cooled reactors HTTR;HTTR-IS plan, Proc. Of ICAPP'06, Reno,US.june 4-8,2006, Paper6024 (2006).

[2] K. Takeno, K. Okabayashi, A. Kouchi, T. Nonaka, K. Hashiguchi, K. Chitose, Dispersion and explosion field tests for 40 MPa pressurized hydrogen, International Journal of Hydrogen Energy, vol.32, pp.2144-2153 (2007).

[3] T. Tanaka, T. Azuma, J. A. Evans, P. M. Cronin, D. M. Johnson, R. P. Cleaver, Experimental study on hydrogen explosions in full-scale hydrogen filling station model, International Journal of Hydrogen Energy, vol.32, pp. 2162-2170 (2007).

[4] M. Groethe, E. Merilo, J. Colton, S. Chiba, Y. Sato, H. Iwabuchi, Large-scale hydrogen deflagrations and detonations, International Journal of Hydrogen Energy, vol.32, pp. 2115-2133 (2007).

[5] S. B. Dorofeev, Evaluation of safety distances related to unconfined hydrogen explosions, International Journal of Hydrogen Energy, vol.32, pp. 2118-2124 (2007).

[6] J. Lobato, P. Cañizares, M. A. Rodrigo, Ch. Sáez, J. J. Linares, A comparison of hydrogen cloud explosion models and the study of the vulnerability of the damage caused by an explosion of H_2, International Journal of Hydrogen Energy, vol.31, pp. 1780-1790 (2006).

[7] Hoi Dick Ng, Yiguang Ju, John H. S. Lee, Assessment of detonation hazards in high-pressure hydrogen storage from chemical sensitivity analysis, International Journal of Hydrogen Energy, vol.32, pp.93-99 (2007).

[8] P. Middha, O. R. Hansen, M. Groethe, B. J. Arntzen, Hydrogen Explosion Study in a Confined Tube: FLACS CFD Simulations and Experiments, 21st ICDERS, July 23-27, 2007, Poiters, France.

[9] Fluent Inc. User's Guide FLUENT 6.3 (2006).

[10] H.Kajino,et.al.,A study on possible hazards by leakage of compressed hydrogen gas, kouatsugasu, Vol.14, No.3, pp127-138 (1977).

[11] R.Tayler, R. Krishna, Multicomponent mass transfer, wiley-interscience, pp242-265 (1993)

Table 2.1 Hydrogen properties

Temperature [K]	100	200	300	400	500	600
c_p [$J.kg^{-1}.K^{-1}$]	11,220	13,530	14,310	14,480	14,520	14,550
λ [$J.m^{-1}.K^{-1}$]	0.0676	0.13	0.181	0.226	0.267	0.358
η [Pa.s]	$4.21 x 10^{-6}$	$6.81 x 10^{-6}$	$8.96 x 10^{-6}$	$1.085 x 10^{-6}$	$1.259 x 10^{-6}$	$1.656 x 10^{-6}$

Table 2.2 Nitrogen properties

Temperature [K]	100	200	300	400	500	600
c_p [$J.kg^{-1}.K^{-1}$]	1,071	1,043	1,041	1,044	1,055	1,074

Temperature [K]	300	400	500	600	700
λ [$J.m^{-1}.K^{-1}$]	0.02598	0.03252	0.03864	0.0441	0.0493
η [Pa.s]	$1.787 x 10^{-5}$	$2.217 x 10^{-5}$	$2.602 x 10^{-5}$	$2.955 x 10^{-5}$	$3.284 x. 10^{-5}$

Table 2.3 Oxygen properties

Temperature [K]	100	200	300	400	600
c_p [$J.kg^{-1}.K^{-1}$]	953	915	920	942	1,003

Temperature [K]	140	200	240	300	400	600
λ [$J.m^{-1}.K^{-1}$]	0.0131	0.0184	0.0217	0.0263	0.0341	0.0486
η [Pa.s]	$1.08 x 10^{-5}$	$1.48 x 10^{-5}$	$1.73 x 10^{-5}$	$2.07 x 10^{-5}$	$2.58 x 10^{-5}$	$3.44 x 10^{-5}$

Table 3.1 Hydrogen concentration changes with distance - experimental and calculated values

Distance x [m]	Mole fraction of hydrogen		
	Experimental	Schmidt num. 0.7	Schmidt num. 1.4
2.01647	0.932513	0.895457	0.972097
3.02847	0.82413	0.75391	0.871406
4.04047	0.727301	0.63421	0.770611
5.05246	0.646053	0.536759	0.682097
6.06446	0.578877	0.465911	0.598522
7.07646	0.523200	0.411311	0.532997
8.08845	0.476659	0.36621	0.478665
9.10045	0.437352	0.327133	0.432817
10	0.407288	0.300827	0.401295

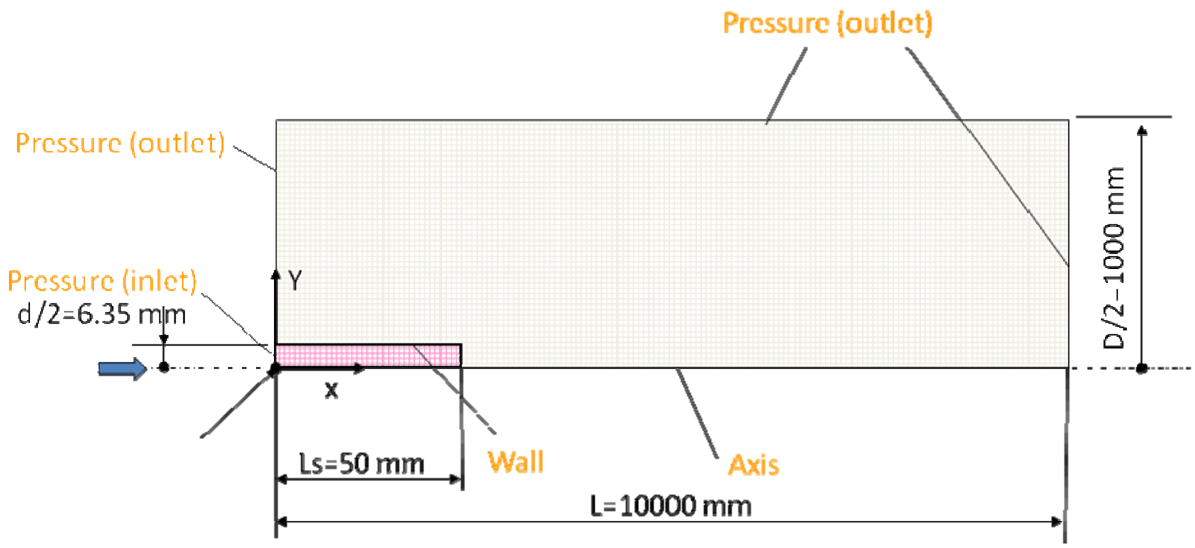

Figure 2.1 2D axisymmetric model with boundary condition (orange color)

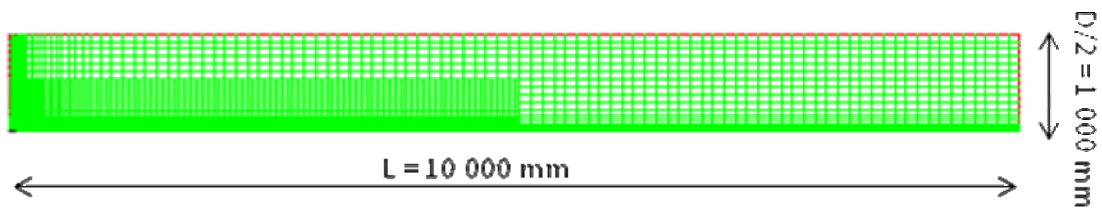

Figure 2.2 Adapted mesh

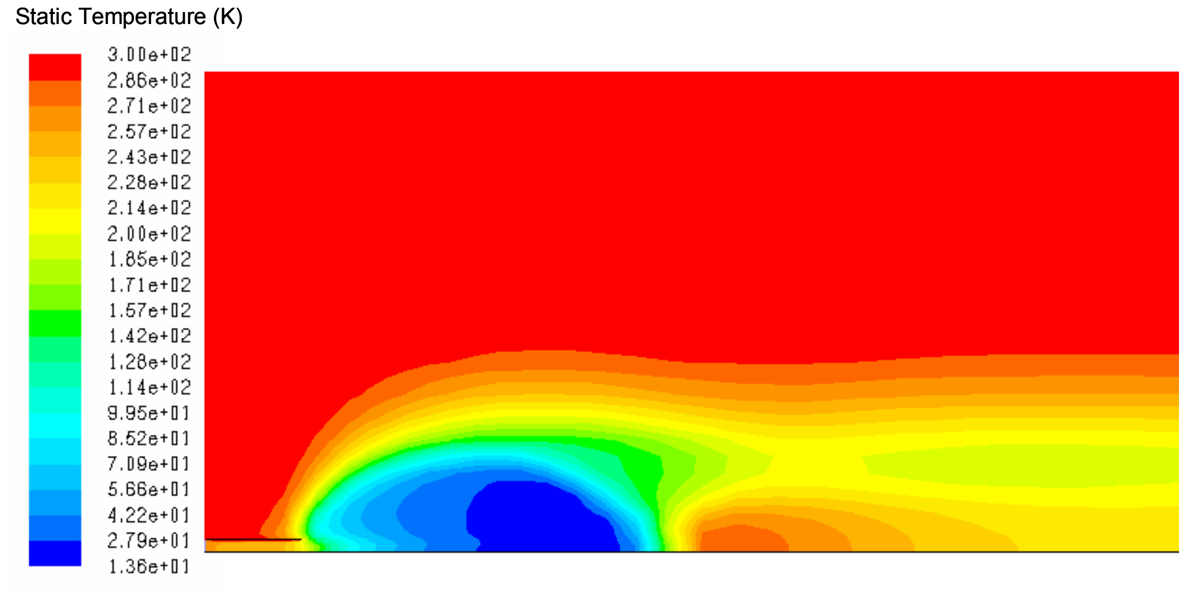

(a) Turbulent Schmidt number 0.7

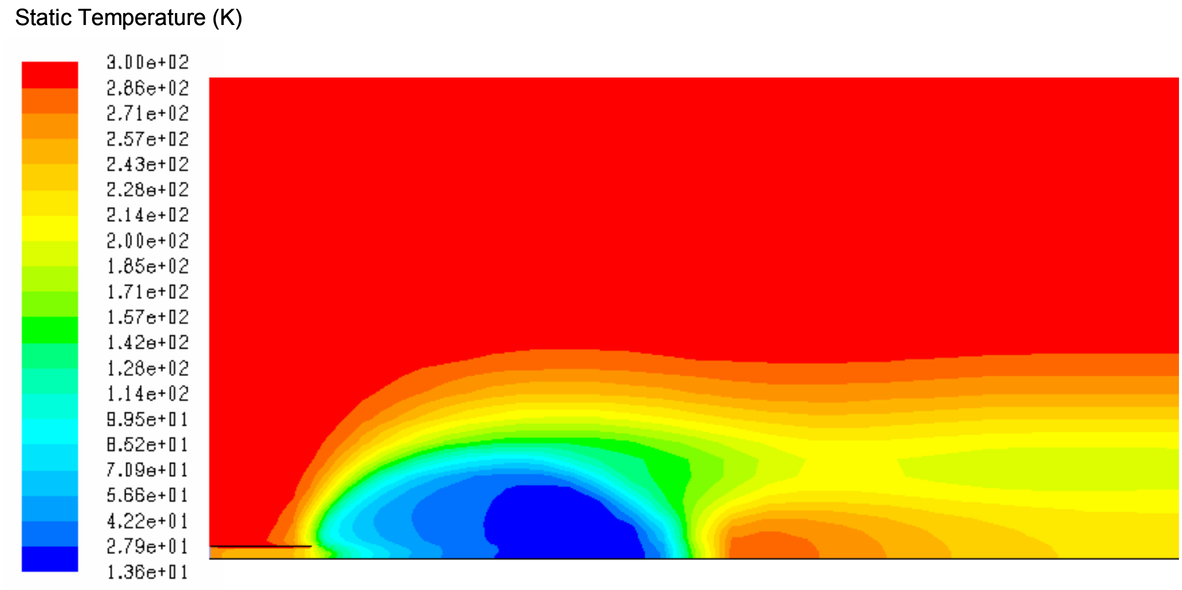

(b) Turbulent Schmidt number 1.4

Figure 3.1 Static temperature distribution around nozzle

This is a blank page

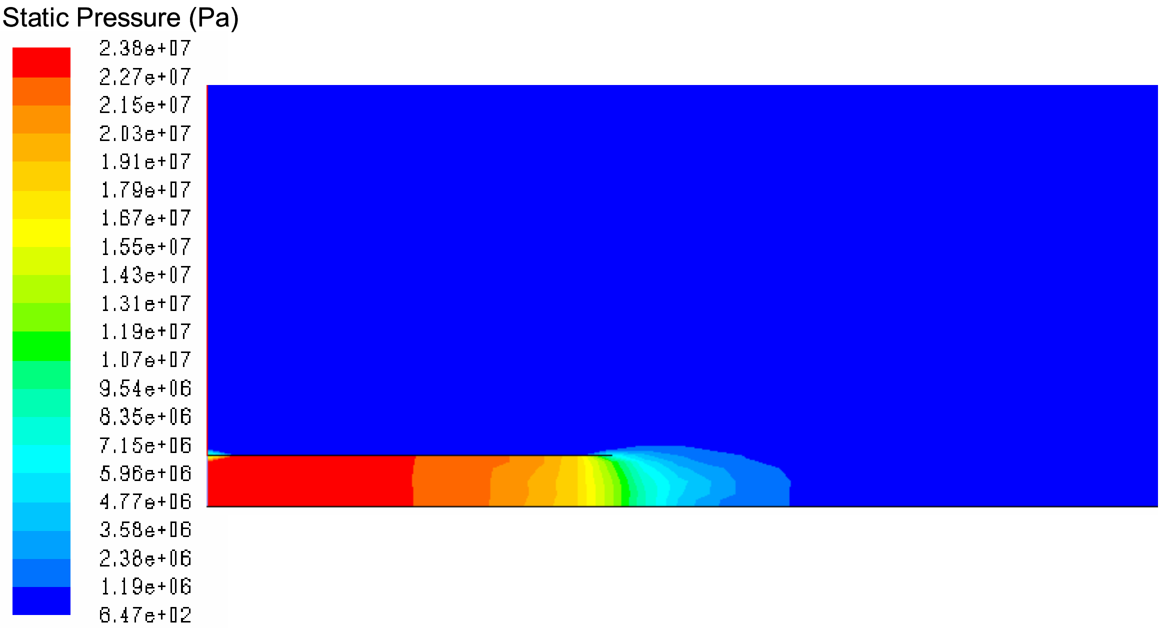

(a) Turbulent Schmidt number 0.7

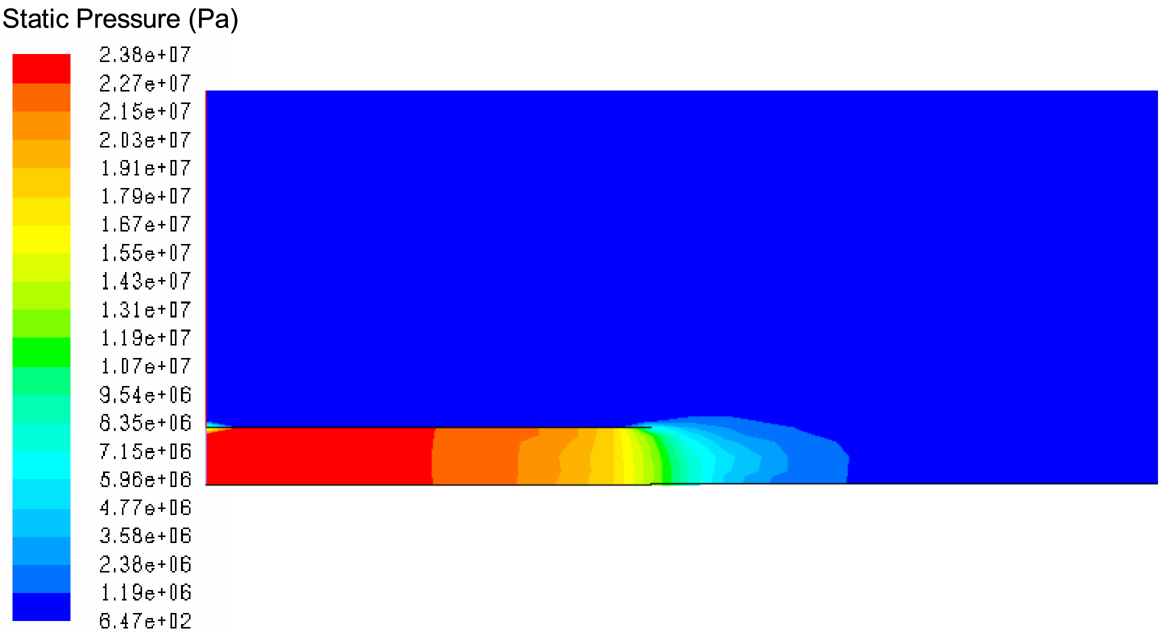

(b) Turbulent Schmidt number 1.4

Figure 3.2 Static pressure distribution around nozzle

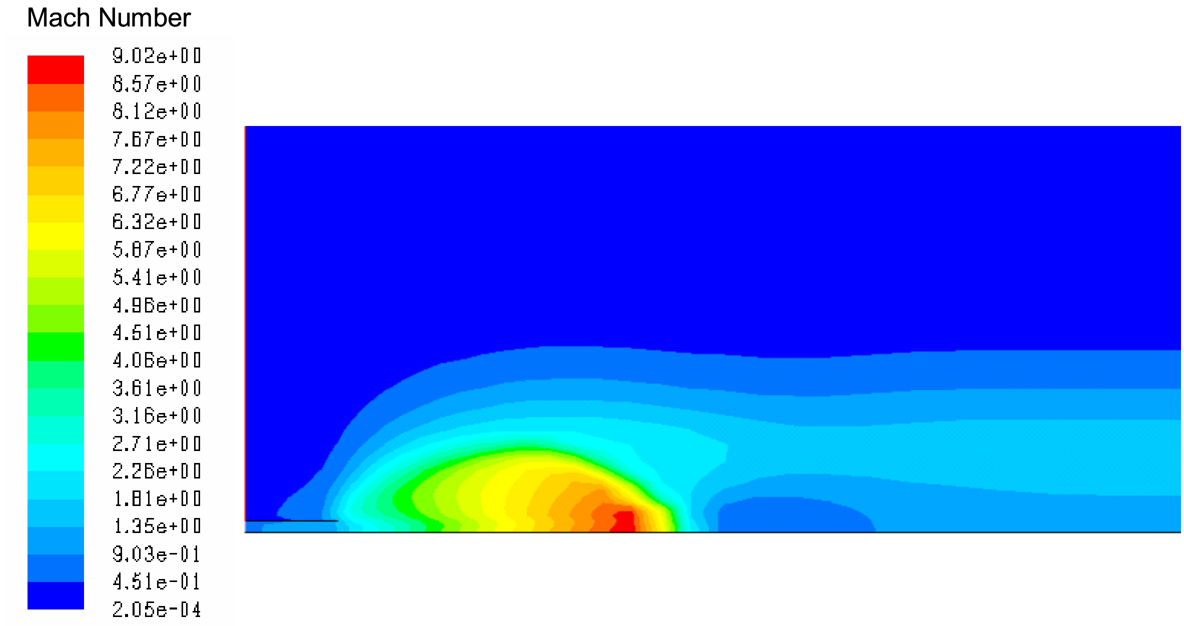

(a) Turbulent Schmidt number 0.7

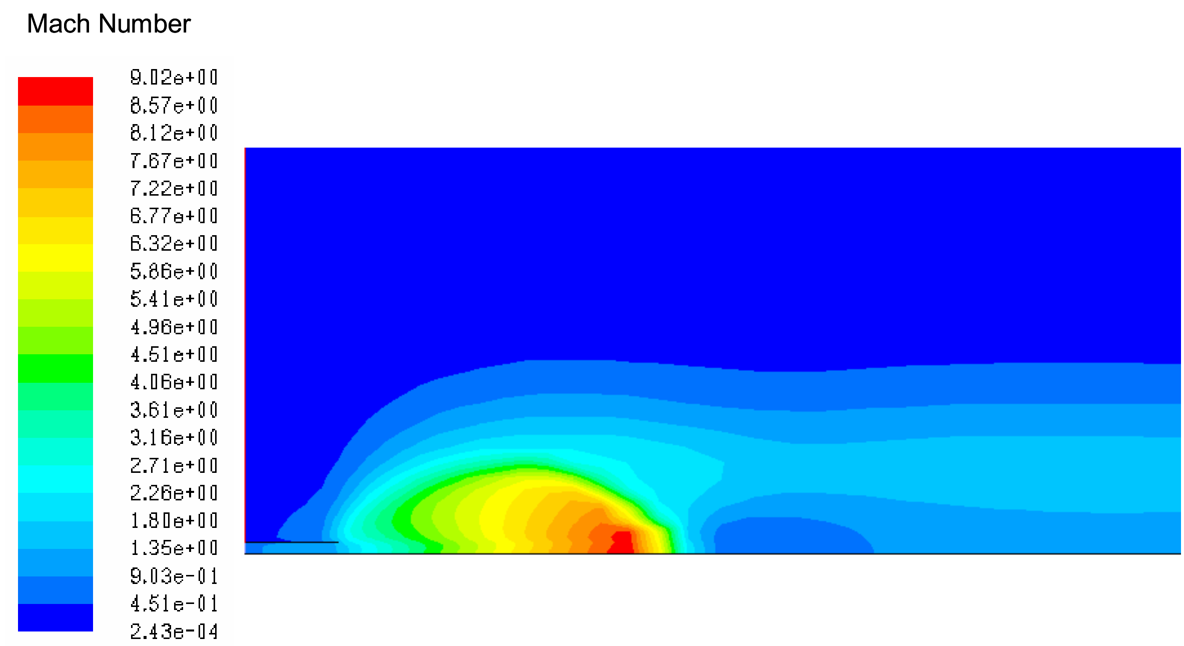

(b) Turbulent Schmidt number 1.4

Figure 3.3 Mach number distribution around nozzle

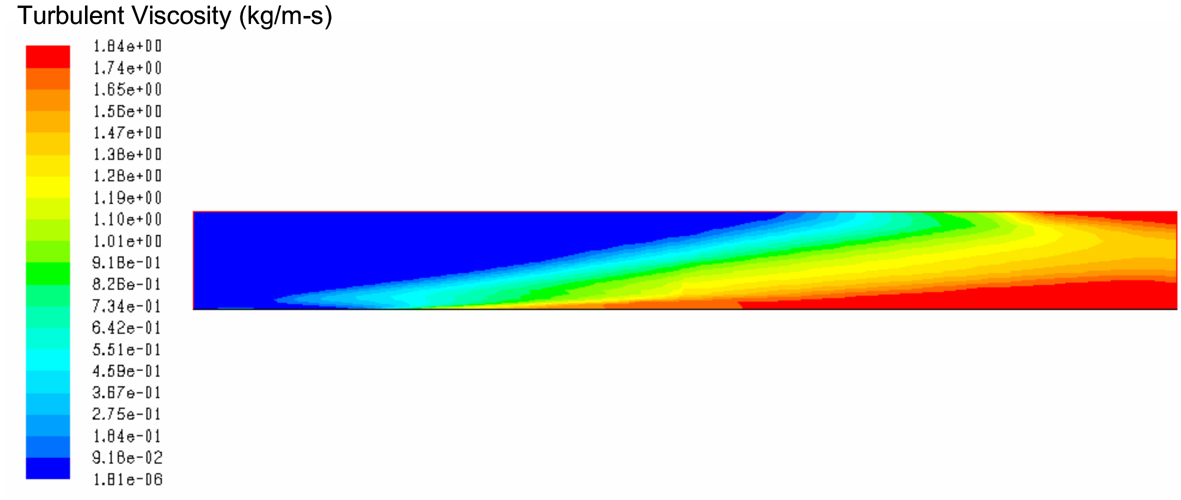

(a) Turbulent Schmidt number 0.7

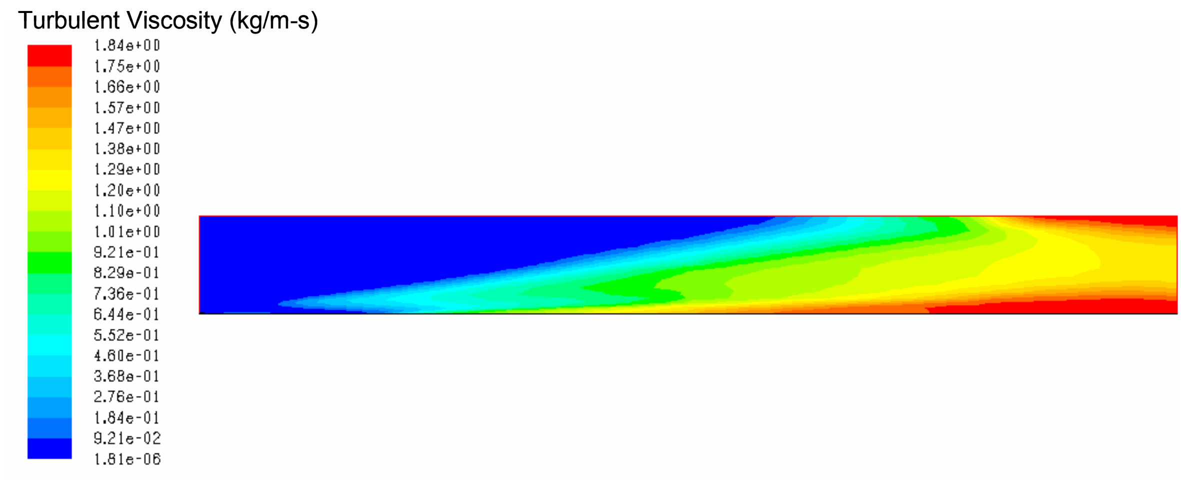

(b) Turbulent Schmidt number 1.4

Figure 3.4 Turbulent viscosity distribution

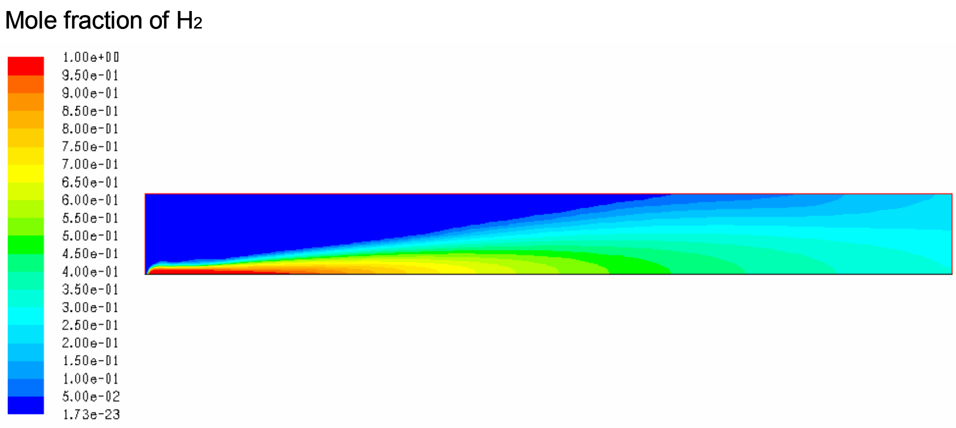

(a) Turbulent Schmidt number 0.7

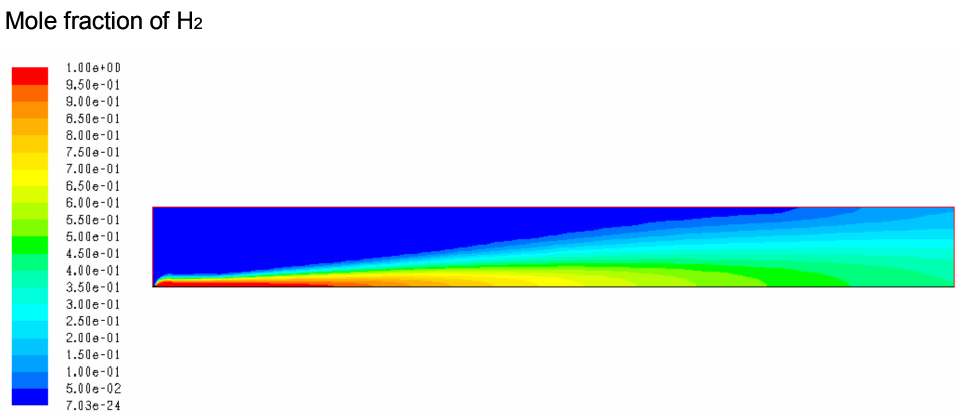

(b) Turbulent Schmidt number 1.4

Figure 3.5 Hydrogen concentration distribution

This is a blank page

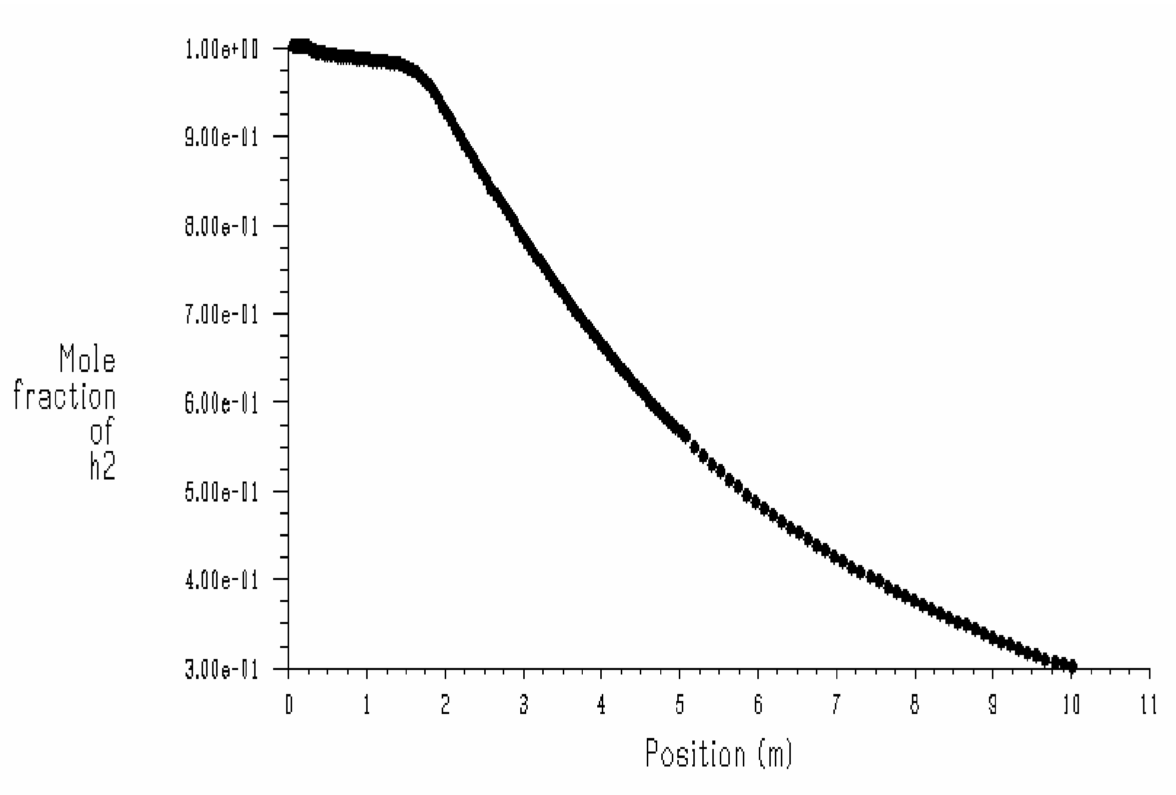

(a) Turbulent Schmidt number 0.7

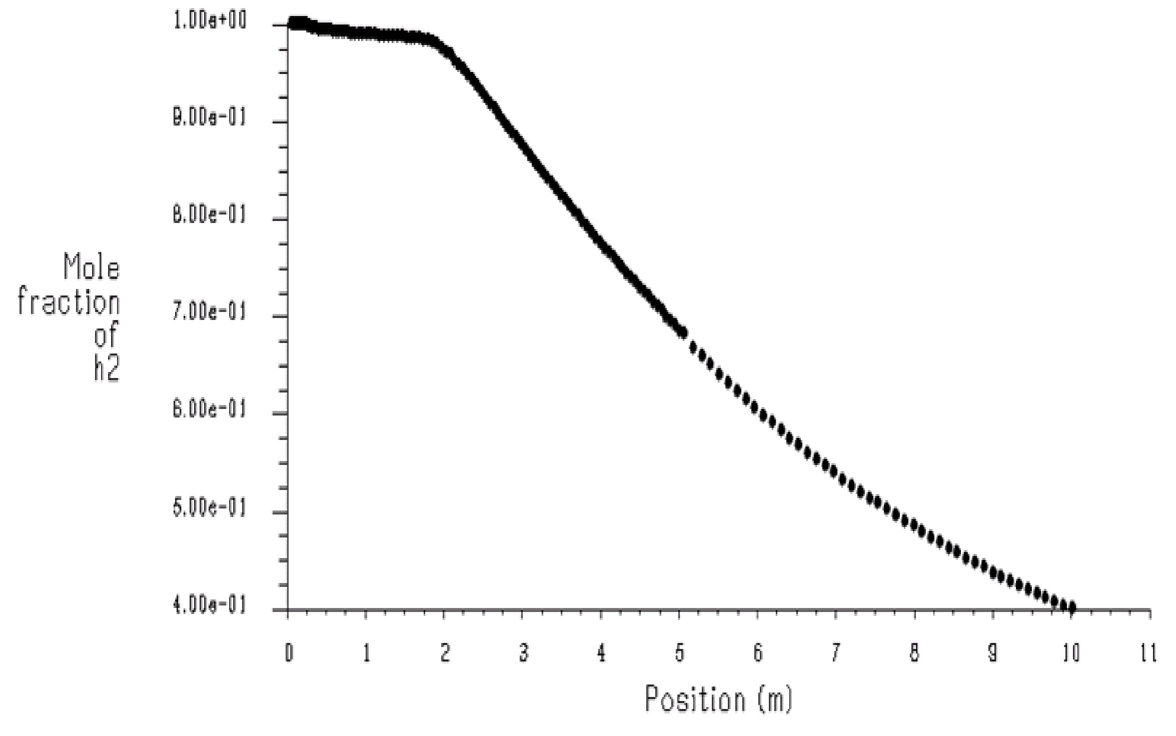

(b) Turbulent Schmidt number 1.4

Figure 3.6 X – Y plot of Hydrogen concentration distribution

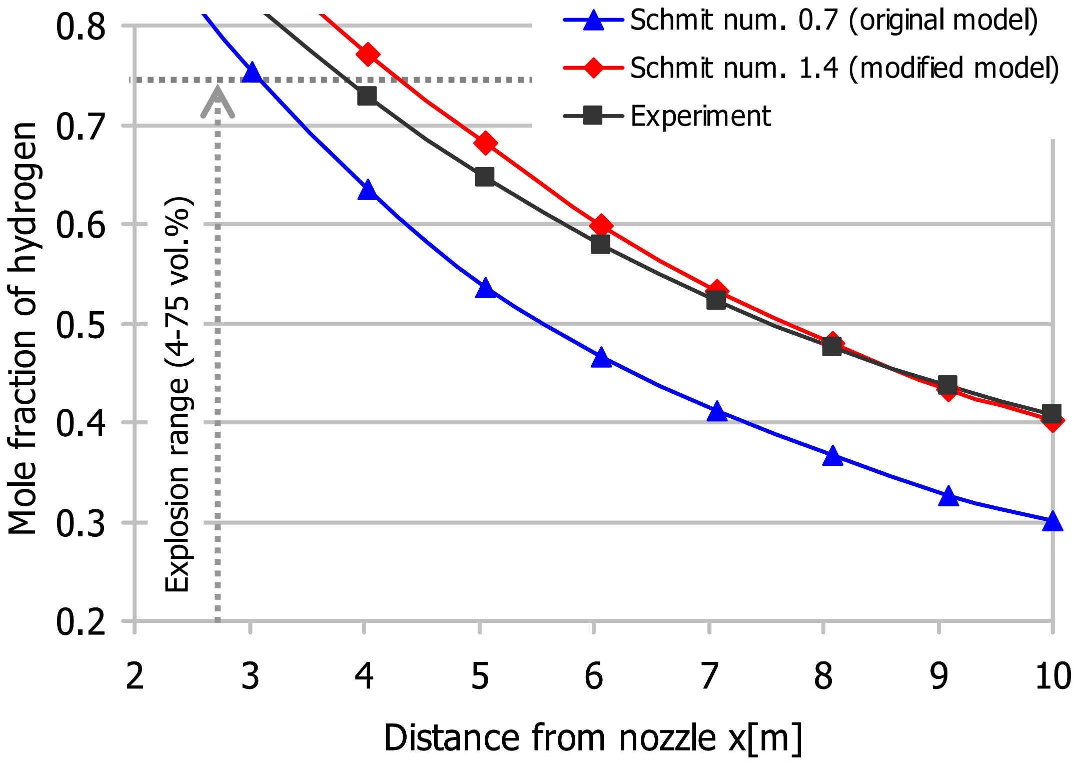

Figure 3.7 Experimental and calculated hydrogen concentrations

This is a blank page

Appendix

Literature survey on hydrogen explosion and detonation experiments and analysis

Introduction

Hydrogen is considered as a future fuel for transportation and stationary use and therefore it is worthwhile to investigate whether we can use hydrogen safely. On that ground a number of experiments and analysis was made considered hydrogen release and dispersion, fire and explosions.

In this literature survey, you can find a list of experiments and analysis on hydrogen explosion and detonation.

A. Literature survey on hydrogen explosion and detonation experiments

Dispersion and explosion field tests for 40 MPa pressurized hydrogen [2]

International Journal of Hydrogen Energy, vol.32, pp.2144-2153 (2007).

K. Takeno[a], K. Okabayashi[a], A. Kouchi[a], T. Nonaka[a], K. Hashiguchi[a], K. Chitose[b]

[a]Mitsubishi Heavy Industries Ltd., Nagasaki R&D center, Technical Headquarters, 5-717-1 Fukahori-machi, Nagasaki 851-0392, Japan

[b]Mitsubishi Heavy Industries Ltd., Nuclear Energy Systems Headquarters, Minatomirai, Nishi-ku, Yokohama 220-8401, Japan

Objective

The objective of this research is to collect data which can be used for the evaluation of standards for hydrogen refueling stations for fuel cell powered vehicles.

Experiment description and conditions

This experiment concerns about hydrogen high pressure storage (40 MPa) and envisions two cases of accidents: 1) a pinhole in equipment representing continuous leakage at a constant mass flow and 2) a rupture of the piping leading to a major leakage in short period. First, the diffusion test were conducted prior to the explosion tests.

Leakage opening	d	0.5 – 10	[mm]
Ignition time (from start of leakage)	t_{ign}	0.5 – 5	[s]
Tank capacity		25 – 100	[Nm^3]
Tank pressure	p_0	10 – 40	[MPa]
Ignition electric spark		20	[mJ]
	0.5 – 7.5 m away from the nozzle, 1 m above the ground		

Results

The rise of the pressure wave is very rapid in terms of deflagration. Leakage velocity has a great effect on explosiveness. The overpressure larger than 20 kPa was measured at 3.9 m from the ignition point at t_{ign}=2 s. Maximum explosive power is TNT=5 kg (t_{ign}=0.85 s, d=10 mm, p_0=40 MPa).

Experimental study on hydrogen explosions in full-scale hydrogen filling station model [3]

International Journal of Hydrogen Energy, vol.32, pp. 2162-2170 (2007).

T. Tanaka[a], T. Azuma[a], J. A. Evans[b], P. M. Cronin[b], D. M. Johnson[b], R. P. Cleaver[b]

[a]Engineering Department, Osaka Gas Co., Ltd., 5-11-61, Torishima, Konohana-ku, Osaka 554-0051, Japan

[b]Advantica Ltd., Ashby Road, Lounghborough, Leicestershire LE11 3GR, UK

Objective

The objective of this research is to investigate the safety aspects of hydrogen refueling stations to establish a suitable safety zone around a station.

Experiment description and conditions

This experimental program consisted of dispersion and explosion experiments in 1) a model chamber and in 2) a model of filling station: a) the storage room and b) the dispenser. In the explosion experiments was studied an overpressure distribution produced by hydrogen explosions.

1) Test chamber

Test chamber volume	22	[m^3]
Test chamber dimensions	8.25x3x2.7	[m]
	front face was open (in some tests also the upper half of two long sidewalls)	
Hydrogen concentration	15, 30, 40, 50	[%]
Ignition electric spark	placed in the center of gas cloud	

Results

The larges overpressure was measured for hydrogen concentration 30 – 40 % = 9.8 kPa. Safety zone depends on hydrogen concentration (and this depends on the release and ventilation conditions)

2) Model of a hydrogen filling station

a) Storage room

Storage room dimensions	5x6x4	[m]
	the top 1 m gap between the roof and the walls	
Hydrogen concentration	8, 15, 26	[%]
High-pressure cylinders capacity	250	[l]
High-pressure cylinders pressure	40	[MPa]

Results

H_2 concentration in room (%)	Maximum overpressure (kPa)	
	Inside room	At station boundary
8	minimal	Not detected
15	0.4 – 1.3	3.1 – 3.4
26	> 100	28 - 111

b) Dispenser

Nozzle diameters	8; 1.6; 0.8	[mm]
Storage vessel capacity	250	[l]
Storage vessel pressure	40	[MPa]
Ignition electric spark	4 m from a nozzle	

Results

The ignition time has a significant effect on the overpressure and the maximum overpressure was measured for 1.2 s (above 9.8 kPa).

Large-scale hydrogen deflagrations and detonations [4]

International Journal of Hydrogen Energy, vol.32, pp. 2115-2133 (2007).

M. Groethe[a], E. Merilo[a], J. Colton[a], S. Chiba[b], Y. Sato[c], H. Iwabuchi[c]

[a]Poulter Laboratory, SRI International, 333 Ravenswood Avenue, Menlo Park, CA 94025, USA

[b]SRI-East Asia, SRI International, Parka Side 8F2, Ichibancho, Chiyoda-ku, Tokyo

102-0082, Japan
[c]R&D Division, IAE, 14-2, Nishishinbashi 1-chome, Minato-ku, Tokyo 105-0003, Japan

Objective

These experiments provide data needed to address accident scenarios and to evaluate numerical models (e.g. AutoReaGas code).

1) 300 m³ experiments

Experiment description and conditions

Facility volume	V	300	[m^3]
	aluminum geodesic dome frame covered with a thin polyethylene film		
Cylinders dimensions	Num.	18	
	d	0.46	[m]
	h	3	[m]
	placed around the ignition point in two rings		
	r_1	1.1	[m]
	r_2	1.9	[m]
Hydrogen concentration		15 – 30	[% vol.]
Ignition point	bottom centre of the facility		
	10 g of C-4		

Results

Overpressure and heat flux were measured in this experiments at a range of 15.61 m from the ignition point.

2) Tunnel experiments

Experiment description and conditions

The tunnel represents a vehicle tunnel at 1/5 scale. There were performed spark-ignited deflagration tests (with or without ventilation).

Tunnel length	78.5	[m]
Tunnel cross-sectional area	3.74	[m^2]

Hydrogen concentration	9.5 – 30	[% vol.]
Hydrogen release	0.1 kg in 20 s and 2.2 kg in 420 s in the centre of tunnel, with (1.6 m^3/s) and without forced ventilation	
Vehicle model dimensions	940x362x 343	[mm]
	placed down the center of the tunnel	

Results

Hydrogen concentration (% vol.)	Pressure pulses (kPa)
9.5 (0.32 kg)	Not detected
20 (0.67 kg)	35
30 (1 kg)	150

B. Literature survey on hydrogen explosion and detonation analyses

Evaluation of safety distances related to unconfined hydrogen explosions [5]

International Journal of Hydrogen Energy, vol.32, pp.2118-2124 (2007).
S. B. Dorofeev
FM Global, 1151 Boston-Providence Turnpike, Norwood, MA 02062, USA

Objective

The objective of this study is to develop a simple approximate method for evaluation of blast effects and safety distances for hydrogen explosions.

Analytical model and conditions

The method includes:

- a model for the evaluation of hydrogen flame speeds,
- a model for properties of "the worst case" hydrogen distribution,
- a model for blast parameters,

  Maximal blast overpressure (P) and positive impulse (I) are a function of distance (R) from the blast epicenter.
- a set of blast damage criteria.

Three hypothetical cases of obstacles surrounding the release location:

- high congestion: distance between obstacles x=0.2 m, size of obstacles y=0.1 m (unit with multiple tubes and pipelines),
- medium congestion: x=1 m, y=2 m (technological unit surrounded by other units),
- low congestion: x=4 m, y=2 m (a large technological unit surrounded with other technological units, e.g. refueling station).

Results

Release of 10 kg of hydrogen do not result in building damages for the case of the low congestion, but it results in building damages for the case of the medium congestion (at distances of up to 40 m). 10 kg hydrogen release for the case of the high congestion is very severe and results in building damages at distances of up to 70 m.
For the different levels of congestion (low, medium, high) were determined the safety

distances defined by minimum damage for buildings.

A comparison of hydrogen cloud explosion models and the study of the vulnerability of the damage caused by an explosion of H_2 [6]

International Journal of Hydrogen Energy, vol.31, pp. 1780-1790 (2006).

J. Lobato, P. Cañizares, M. A. Rodrigo, Ch. Sáez, J. J. Linares

Faculty of Chemistry, Department of ChemicalEngineering, University of Castilla – La Mancha. Campus Universitarios/n. 13004. Ciudad Real, Spain

Objective

The objective of this study is to provide a an easy tool for estimation the effects of an unconfined hydrogen cloud explosion as a function of distance. For this purpose it was used three prediction models – TNT equivalency explosion model, TNO multi-energy model, and Baker-Strehlow-Tang model (BST).

Analytical model and conditions

Hydrogen cylinders: 2x60 dm^3 with 8.8 m^3 of hydrogen,
Hydrogen pressure: 200 bar,
Hole in a pipe: d=1 mm, leakage time2h before explosion,
Laboratory dimension: 11x8x3 m.

TNT equivalency explosion model: first, the fraction of total energy of explosion used in the shock wave is calculated. Than, it is converted into the equivalent mass of TNT

$$W_{TNT} = \frac{W_{gas}\eta\Delta H_{c(gas)}}{\Delta H_{c(TNT)}}$$

W_{TNT} (kg) is the equivalent mass of TNT that produce the same effects as the explosion, η is the explosion yield, W_{gas} is the total mass of flammable gas, $\Delta H_{c(gas)}$ (kJ/kg) is the lower heat of combustion of material, $\Delta H_{c(TNT)}$ (kJ/kg) is the heat of combustion of TNT.

TNO multi-energy model: based on premise a vapor cloud explosion occurs only within a partially confined area of flammable vapor. The model is represented as homogenous, stoichiometric mixture hemispherical cloud with a combustion energy $3.1.10^6$ J/m^3 (the average heat of combustion of mixture of hydrogen and air). Results are given as a family of curves, which represent the range of severities (from deflagrations to detonations).

Baker-Strehlow-Tang model: this model also uses a family of curves to relate overpressure to energy scaled distance.

<u>**Results**</u>

The TNT model predicts higher overpressure than the other two models. TNO and BST models predict similar overpressure except areas at very low distances.

Assessment of detonation hazards in high-pressure hydrogen storage from chemical sensitivity analysis [7]

International Journal of Hydrogen Energy, vol.32, pp.93-99 (2007).

Hoi Dick Ng[a], Yiguang Ju[a], John H. S. Lee[b]

[a]Department of Mechanical and AerospaceEngineering, Princeton University, Princeton, NJ 08544, USA

[b]Department of Mechanical Engineering, McGill University, Montréal, Québec, Canada

<u>**Objective**</u>

The objective of this study is to assess a detonation sensitivity of hydrogen-air mixture using kinetic mechanism of hydrogen combustion. This will be helpful for preventing a possible explosion in a high-pressure hydrogen storage facilities when contaminated with air.

<u>**Analytical model and conditions**</u>

The accurate detailed chemical kinetics model is used in this study to quantify the effect of initial pressure on the hydrogen – air detonation sensitivity. The characteristic cell size is considered as a characteristic parameter of detonation sensitivity of mixture:

$$\chi = \varepsilon_I \frac{\Delta_I}{\Delta_R} = \varepsilon_I \Delta_I \frac{\sigma_{\max}}{u'_{CJ}}$$

Table 1 Coefficients of detonation cell size with N=3

Coefficients	Values
A_0	30.465860763763

a_1	89.55438805808153
a_2	-130.792822369483
a_3	42.02450507117405
b_1	-0.02929128383850
b_2	$1.026325073064710.10^{-5}$
b_3	$-1.031921244571857.10^{-9}$

It is expected cell sizes decrease with increasing initial pressure (probability of detonation increases with pressure). Hydrogen – air mixture does not follow this trend and is not more sensitive than any other hydrocarbon – air mixture at elevated initial pressure.

When the cell size is known it is possible to determine the critical initiation energy for hydrogen – air mixture detonation:

$$R = \left(\frac{E_{source}}{\alpha_2 \rho_0}\right)^{\frac{1}{3}} \left(\frac{2}{5}\frac{1}{U}\right)^{\frac{2}{3}} \exp\left(\frac{\beta_2 Q}{3U^2}\right)$$

E_{source}	Critical direct initiation energy
R	Critical radius (the first explosion bubbles observed)
Q	Heat of reaction
U	Shock velocity
ρ_0	Initial density
α_2	Constant, $0.31246\ (\gamma-1)^{-1.1409-0.11735\log10(\gamma-1)}$
β_2	Constant, $4.1263\ (\gamma-1)^{1.2530+0.14936\log10(\gamma-1)}$
γ	Specific heat ratio in mixture

Results

The boundary between fast and slow branching regimes for hydrogen – air mixture (T_0 = 300 K)was established on initial pressure $p_0 \approx 4$ atm. The chemical kinetics above this pressure is characterized by low branching reaction and small energy release rate. This implies that hydrogen – air mixture at elevated initial pressure is lowly detonation sensitive.

The critical direct initiation energy increases with increasing initial pressure (this again implies mixture is less sensitive at elevated pressure).

In conclusion, the probability of hydrogen – air mixture detonation at elevated initial pressure is not higher than in other hydrocarbon fuels.

Hydrogen Explosion Study in a Confined Tube: FLACS CFD Simulations and Experiments [8]

21st ICDERS, July 23-27, 2007, Poiters, France

P. Middha[a,c], O. R. Hansen[a], M. Groethe[b], B. J. Arntzen[a,c]

[a]GexCon AS, P.O. Box 6015, Postterminalen, NO-5892 Bergen, Norway

[b]SRI International, Poulter Laboratory, 333 Ravenswood Avenue, Menlo Park, CA 94025, USA

[c]University of Bergen,Department of Physics and Technology, Allégaten 55, NO-5007 Bergen, Norway

Objective

The objective of this paper is to compare results of numerical simulations and experiments of deflagration a tube geometry (10 m long tube with square section) using the CFD tool FLACS and also investigate the possibilities of deflagration to detonation transition occurrence.

Experiment description and conditions

The experimental facility consisted of 9.9 m long steel tube with square section (dimension 38.1 cm) inside the tube were installed different obstacle (6.35 cm thick, 11.43, 16.51, and 22.86 cm high, spacing between blocks 38.1, 76.2, or 152.4 cm) to induce turbulence. The first block was always located at 38.1 cm from the initiation end. (more about the experiment: M. Groethe, J. Colton, S. Chiba. Hydrogen deflagration safety studies in a confined tube. 14th World Hydrogen Energy Conference, Montreal, Québec, Canada, June 9 – 13, 2002)

Results

The simulations of hydrogen deflagration compare reasonably well with experimental predictions. Very high overpressure (15 – 20 bar) and fast flames makes possible to deflagration to detonation transition. The simulations indicated a deflagration to detonation transition (DDT) at 4 – 5 m from ignition point for hydrogen concentration of 30 % and obstacles 11.43 cm high. DDT was indicated at 3 m from ignition for obstacles 22.86 cm high. Other results are not presented because FLACS lacks a shock ignition model and detonation front cannot propagate.

国際単位系（SI）

表１．SI 基本単位

基本量	SI 基本単位	
	名称	記号
長さ	メートル	m
質量	キログラム	kg
時間	秒	s
電流	アンペア	A
熱力学温度	ケルビン	K
物質量	モル	mol
光度	カンデラ	cd

表２．基本単位を用いて表されるSI組立単位の例

組立量	SI 基本単位	
	名称	記号
面積	平方メートル	m^{2}
体積	立法メートル	m^{3}
速さ，速度	メートル毎秒	m/s
加速度	メートル毎秒毎秒	m/s^{2}
波数	毎メートル	m-1
密度（質量密度）	キログラム毎立法メートル	kg/m^{3}
質量体積（比体積）	立法メートル毎キログラム	m^{3}/kg
電流密度	アンペア毎平方メートル	A/m^{2}
磁界の強さ	アンペア毎メートル	A/m
（物質量の）濃度	モル毎立方メートル	mol/m^{3}
輝度	カンデラ毎平方メートル	cd/m^{2}
屈折率	（数の）1	1

表５．SI 接頭語

乗数	接頭語	記号	乗数	接頭語	記号
10^{24}	ヨタ	Y	10^{-1}	デシ	d
10^{21}	ゼタ	Z	10^{-2}	センチ	c
10^{18}	エクサ	E	10^{-3}	ミリ	m
10^{15}	ペタ	P	10^{-6}	マイクロ	µ
10^{12}	テラ	T	10^{-9}	ナノ	n
10^{9}	ギガ	G	10^{-12}	ピコ	p
10^{6}	メガ	M	10^{-15}	フェムト	f
10^{3}	キロ	k	10^{-18}	アト	a
10^{2}	ヘクト	h	10^{-21}	ゼプト	z
10^{1}	デカ	da	10^{-24}	ヨクト	y

表３．固有の名称とその独自の記号で表されるSI組立単位

組立量	SI 組立単位			
	名称	記号	他のSI単位による表し方	SI基本単位による表し方
平面角	ラジアン[a]	rad		m・m^{-1}=1[b]
立体角	ステラジアン[a]	sr[c]		m^{2}・m^{-2}=1[b]
周波数	ヘルツ	Hz		s^{-1}
力	ニュートン	N		m・kg・s^{-2}
圧力，応力	パスカル	Pa	N/m^{2}	m^{-1}・kg・s^{-2}
エネルギー，仕事，熱量	ジュール	J	N・m	m^{2}・kg・s^{-2}
工率，放射束	ワット	W	J/s	m^{2}・kg・s^{-3}
電荷，電気量	クーロン	C		s・A
電位差（電圧），起電力	ボルト	V	W/A	m^{2}・kg・s^{-3}・A^{-1}
静電容量	ファラド	F	C/V	m^{-2}・kg^{-1}・s^{4}・A^{2}
電気抵抗	オーム	Ω	V/A	m^{2}・kg・s^{-3}・A^{-2}
コンダクタンス	ジーメンス	S	A/V	m^{-2}・kg^{-1}・s^{3}・A^{2}
磁束	ウエーバ	Wb	V・s	m^{2}・kg・s^{-2}・A^{-1}
磁束密度	テスラ	T	Wb/m^{2}	kg・s^{-2}・A^{-1}
インダクタンス	ヘンリー	H	Wb/A	m^{2}・kg・s^{-2}・A^{-2}
セルシウス温度	セルシウス度[d]	℃		K
光束	ルーメン	lm	cd・sr[c]	m^{2}・m^{-2}・cd=cd
照度	ルクス	lx	lm/m^{2}	m^{2}・m^{-4}・cd=m^{-2}・cd
（放射性核種の）放射能	ベクレル	Bq		s^{-1}
吸収線量，質量エネルギー分与，カーマ	グレイ	Gy	J/kg	m^{2}・s^{-2}
線量当量，周辺線量当量，方向性線量当量，個人線量当量，組織線量当	シーベルト	Sv	J/kg	m^{2}・s^{-2}

(a) ラジアン及びステラジアンの使用は、同じ次元であっても異なった性質をもった量を区別するときの組立単位の表し方として利点がある。組立単位を形作るときのいくつかの用例は表４に示されている。
(b) 実際には、使用する時には記号rad及びsrが用いられるが、習慣として組立単位としての記号“１”は明示されない。
(c) 測光学では、ステラジアンの名称と記号srを単位の表し方の中にそのまま維持している。
(d) この単位は、例としてミリセルシウス度m℃のようにSI接頭語を伴って用いても良い。

表４．単位の中に固有の名称とその独自の記号を含むSI組立単位の例

組立量	SI 組立単位		
	名称	記号	SI 基本単位による表し方
粘度	パスカル秒	Pa・s	m^{-1}・kg・s^{-1}
力のモーメント	ニュートンメートル	N・m	m^{2}・kg・s^{-2}
表面張力	ニュートン毎メートル	N/m	kg・s^{-2}
角速度	ラジアン毎秒	rad/s	m・m^{-1}・s^{-1}=s^{-1}
角加速度	ラジアン毎平方秒	rad/s^{2}	m・m^{-1}・s^{-2}=s^{-2}
熱流密度，放射照度	ワット毎平方メートル	W/m^{2}	kg・s^{-3}
熱容量，エントロピー	ジュール毎ケルビン	J/K	m^{2}・kg・s^{-2}・K^{-1}
質量熱容量（比熱容量），質量エントロピー	ジュール毎キログラム毎ケルビン	J/(kg・K)	m^{2}・s^{-2}・K^{-1}
質量エネルギー（比エネルギー）	ジュール毎キログラム	J/kg	m^{2}・s^{-2}・K^{-1}
熱伝導率	ワット毎メートル毎ケルビン	W/(m・K)	m・kg・s^{-3}・K^{-1}
体積エネルギー	ジュール毎立方メートル	J/m^{3}	m^{-1}・kg・s^{-2}
電界の強さ	ボルト毎メートル	V/m	m・kg・s^{-3}・A^{-1}
体積電荷	クーロン毎立方メートル	C/m^{3}	m^{-3}・s・A
電気変位	クーロン毎平方メートル	C/m^{2}	m^{-2}・s・A
誘電率	ファラド毎メートル	F/m	m^{-3}・kg^{-1}・s^{4}・A^{2}
透磁率	ヘンリー毎メートル	H/m	m・kg・s^{-2}・A^{-2}
モルエネルギー	ジュール毎モル	J/mol	m^{2}・kg・s^{-2}・mol^{-1}
モルエントロピー，モル熱容量	ジュール毎モル毎ケルビン	J/(mol・K)	m^{2}・kg・s^{-2}・K^{-1}・mol^{-1}
照射線量（Ｘ線及びγ線）	クーロン毎キログラム	C/kg	kg^{-1}・s・A
吸収線量率	グレイ毎秒	Gy/s	m^{2}・s^{-3}
放射強度	ワット毎ステラジアン	W/sr	m^{4}・m^{-2}・kg・s^{-3}=m^{2}・kg・s^{-3}
放射輝度	ワット毎平方メートル毎ステラジアン	W/(m^{2}・sr)	m^{2}・m^{-2}・kg・s^{-3}=kg・s^{-3}

表６．国際単位系と併用されるが国際単位系に属さない単位

名称	記号	SI 単位による値
分	min	1 min=60s
時	h	1h =60 min=3600 s
日	d	1 d=24 h=86400 s
度	°	1°=(π/180) rad
分	’	1’=(1/60)°=(π/10800) rad
秒	”	1”=(1/60)’=(π/648000) rad
リットル	l、L	1l=1 dm^{3}=10^{-3}m^{3}
トン	t	1t=10^{3} kg
ネーパ	Np	1Np=1
ベル	B	1B=(1/2)ln10(Np)

表７．国際単位系と併用されこれに属さない単位でSI単位で表される数値が実験的に得られるもの

名称	記号	SI 単位であらわされる数値
電子ボルト	eV	1eV=1.60217733(49)×10^{-19}J
統一原子質量単位	u	1u=1.6605402(10)×10^{-27}kg
天文単位	ua	1ua=1.49597870691(30)×10^{11}m

表８．国際単位系に属さないが国際単位系と併用されるその他の単位

名称	記号	SI 単位であらわされる数値
海里		1海里=1852m
ノット		1ノット=1海里毎時=(1852/3600)m/s
アール	a	1a=1 dam^{2}=10^{2}m^{2}
ヘクタール	ha	1ha=1 hm^{2}=10^{4}m^{2}
バール	bar	1bar=0.1MPa=100kPa=1000hPa=10^{5}Pa
オングストローム	Å	1Å=0.1nm=10^{-10}m
バーン	b	1b=100fm^{2}=10^{-28}m^{2}

表９．固有の名称を含むCGS組立単位

名称	記号	SI 単位であらわされる数値
エルグ	erg	1 erg=10^{-7} J
ダイン	dyn	1 dyn=10^{-5}N
ポアズ	P	1 P=1 dyn・s/cm^{2}=0.1Pa・s
ストークス	St	1 St =1cm^{2}/s=10^{-4}m^{2}/s
ガウス	G	1 G ≙10^{-4}T
エルステッド	Oe	1 Oe ≙(1000/4π)A/m
マクスウェル	Mx	1 Mx ≙10^{-8}Wb
スチルブ	sb	1 sb =1cd/cm^{2}=10^{4}cd/m^{2}
ホト	ph	1 ph=10^{4}lx
ガル	Gal	1 Gal =1cm/s^{2}=10^{-2}m/s^{2}

表10．国際単位に属さないその他の単位の例

名称	記号	SI 単位であらわされる数値
キュリー	Ci	1 Ci=3.7×10^{10}Bq
レントゲン	R	1 R = 2.58×10^{-4}C/kg
ラド	rad	1 rad=1cGy=10^{-2}Gy
レム	rem	1 rem=1 cSv=10^{-2}Sv
X線単位		1X unit=1.002×10^{-4}nm
ガンマ	γ	1γ=1 nT=10^{-9}T
ジャンスキー	Jy	1 Jy=10^{-26}W・m^{-2}・Hz^{-1}
フェルミ		1 fermi=1 fm=10^{-15}m
メートル系カラット		1 metric carat = 200 mg = 2×10^{-4}kg
トル	Torr	1 Torr = (101 325/760) Pa
標準大気圧	atm	1 atm = 101 325 Pa
カロリー	cal	
ミクロン	µ	1 µ =1µm=10^{-6}m

（第７版，1998年改訂）